Optical and Quantum Electronics (2023) 55:982
https://doi.org/10.1007/s11082-023-05230-9

Modification and development of the structural, linear/nonlinear optical and electrical characterization of PVC incorporated with iron chromium oxide and TPAI

A. M. El-naggar[1] · Zein K. Heiba[2] · A. M. Kamal[3] · Mohamed Bakr Mohamed[2]

Received: 19 May 2023 / Accepted: 25 July 2023 / Published online: 9 September 2023
© The Author(s), under exclusive licence to Springer Science+Business Media, LLC, part of Springer Nature 2023

Abstract

PVC/$FeCr_2O_4$/x wt% tetrapropylammonium iodide (TPAI, $x=0$, 2.5, 5, 10, 20) polymers were prepared using casting and sol gel methods. Rietveld refinement was used to determine the structural and microstructural properties of $FeCr_2O_4$ nanofiller. XRD, FTIR, and SEM techniques were applied to explore the effect of fillers on the structural features of PVC polymer. The effect of $FeCr_2O_4$ and/or TPAI on the linear/nonlinear optical properties of PVC was explored. Absorbance was obviously enhanced, and transmittance reduced in the range 200–450 nm upon doping with TPAM. The refractive index and reflectance were increased by loading $FeCr_2O_4$. The direct (4.25 eV) and indirect (4.1 eV) bandgap values of the pure PVC were reduced to 4.21 and 3.95 eV upon loading with $FeCr_2O_4$; both reduced further, but irregularly, as the amount of TPAI increased attaining lowest values 3.11 and 2.62 eV for TPAI content 2.5 wt%. The optical conductivity and the dielectric constant were greatly enhanced by TPAI doping, while the nonlinear optical parameters were improved by $FeCr_2O_4$ loading. Under different excitation wavelengths, the fluorescence intensity was quenched upon loading $FeCr_2O_4$, then reduced a little by adding TPAI; the corresponding CIE chromaticity diagrams were obtained.

Keywords PVC · $FeCr_2O_4$ · TPAI ratios · Structural, optical, dielectric

✉ Zein K. Heiba
zein_kh@yahoo.com

✉ Mohamed Bakr Mohamed
mbm1977@yahoo.com

A. M. El-naggar
amelnaggar@yahoo.com

A. M. Kamal
amgadmazhar@yahoo.com

[1] Research Chair of Exploitation of Renewable Energy Applications in Saudi Arabia, Physics and Astronomy Department, College of Science, King Saud University, P.O. Box 2455, 11451 Riyadh, Saudi Arabia

[2] Physics Department, Faculty of Science, Ain Shams University, Cairo, Egypt

[3] Physics and Astronomy Department, College of Science, King Saud University, P.O. Box 2455, 11451 Riyadh, Saudi Arabia

1 Introduction

Many scientists around the world are focusing their attention on enhancing and characterizing the properties of polymer composites because of the benefits they offer in a variety of optoelectronic applications (El-naggar et al. 2023a, a, b, b, c). Lightweight, low-cost, easily dispersed in water, and quick to prepare are just some of the many impressive properties' polymers possess (El-Naggar et al. 2023a, a, b, b, c). Recently, there has been a need for research into nanofiller-based polymer nanocomposites with high dielectric properties for applications involving energy storage (Bera et al. 2023).

Poly (vinyl chloride) (PVC) has attracted a lot of interest because of its versatile applications and high-quality physicochemical properties. Hydrophobicity, inflammability, formulation flexibility, and low cost are just a few of these advantages (Suvaran et al. 2022).

To create advanced flexible optoelectronic technologies, oxides, sulfides, metal salts and/or iodides materials can be used as filler materials. For example, Ragab et al. incorporated nano ZnO/TiO_2 in polyethylene oxide/carboxymethyl cellulose blend (Ragab 2023). By incorporating toluidine blue dye as an efficient laser optical limiter into polyvinyl alcohol (PVA) composite films, Mohamed et al. developed a smart optical sensor with enhanced conductivity and dielectric properties (Mohammed et al. 2022). Rechargeable batteries, such as lithium and nickel-cadmium (Ni–Cd) polymer batteries, have seen a rise in demand and widespread use due to the growing portable power needs of electronic and medical devices over the past decade. Yassin et al. found that (PVA–PVP)/(Ni–Cd) composite can be used in manufacturing (Ni–Cd) batteries and energy storage devices (Yassin 2020).

Dielectric data for PVC/PVP/$ZnFe_2O_4$ polymers showed that increasing amounts of $ZnFe_2O_4$ decreased the dielectric constant values of the composite. Additionally, the DC conductivity values dropped as $ZnFe_2O_4$-polymer resistance increased with increasing zinc ferrite contents up to 15.0 wt% (Alhulw et al. 2021). The optical dielectric constants and optical conductivity of the polymer both increase with increasing amounts of $Cd_{0.5}Zn_{0.5}Fe_2O_4$ in the PVA matrix (Soliman and Abouhaswa 2020). Depending on the amount of manganese doped into Cd-ferrite, the direct energy gap and other optical parameters change in nanocomposite samples of $Cd_{1-x}Mn_xFe_2O_4$/poly (methyl methacrylate) (PMMA) (Heiba et al. 2020).

To protect against electromagnetic interference (EMI), near-infrared (NIR), and thermal imaging cameras, Anum et al. (2021). Doping a PVA/PEG blend with methyl blue dye improved its luminescence, structural, and dielectric features. The PVC/Cu/Cu_2O nanocomposite films' improved dielectric and optical properties make them a good option for use in energy storage devices (Abdel Maksoud et al. 2023). Doping virgin PVC/PMMA with nano Li4Ti_5O_{12} improved their electrical characteristics. $Li_4Ti_5O_{12}$/PVC/PMMA blends can be employed in different electrochemical and industrial fields such as Li-ion batteries (Al-Muntaser et al. 2020). Al_2O_3/PVC or NiO/PVC composite is found to have an increase in nonlinear refractive index and third-order nonlinear optical susceptibility with increasing Al_2O_3 or NiO amounts, which makes these films suitable for optical device technology (Taha 2019; Taha et al. 2019). By incorporating suitable amounts of I_2 nanofiller into the PVC polymeric matrix, the optical, chemical, and thermal features of PVC-I_2 thin films can be dramatically altered (Telfah et al. 2022a, b). As the percentage of I_2 in polyethylene oxide polymer rises, the optical band gap energy decreases and the refractive index rises (Telfah et al. 2022a, b).

Oxides with a spinel structure are commonly used as practical and low-cost sensors for detecting toxic and hazardous materials. $FeCr_2O_4$ is one of the most significant spinel compounds because of its potential uses. $FeCr_2O_4$ exhibited multiferroic properties (Singh et al. 2011). Furthermore, high theoretical capacity, environmental friendliness, a high abundance, a wide volume variation, and low electronic conductivity are all characteristics of Cr-based ferrite ($CrFe_2O_4$) nanoparticles (Mubasher et al. 2020).

Furthermore, large cations (for example, TEA^+, TBA^+, TPA^+) in tetraethylammonium iodide (TEAI, $C_8H_{20}IN$), tetrabutylammonium iodide (TBAI, $C_{16}H_{36}IN$) and tetrapropylammonium iodide (TPAI, $C_{12}H_{28}IN$) salts are accountable for separating the polymer matrix, creating more space for the movement of smaller cations (Na^+, Li^+, K^+, Ca^{2+}) and iodide ions (Khan et al. 2017). Dye-sensitized solar cells (DSSCs) will operate more effectively with iodide anions that have a higher energy (Yee et al. 2020).

Due to its simplicity, low cost, and concession of control of structure and properties, the sol-gel route is a convenient method for producing nano ferrite (Dippong et al. 2021). In addition, solution casting procedure is the most prominent, effective and cheap technique to manufacture films at laboratory-scale.

For potential use in optoelectronics and in energy storge systems, this work investigates how nano $FeCr_2O_4$ doping and the changing of the TPAI dopant level affects the PVC's optical and electrical characteristics.

2 Methods and materials

$FeCr_2O_4$ was prepared by dissolving stoichiometric amounts from iron(III) nitrate nonahydrate ($Fe(NO_3)_3{\cdot}9H_2O$, Sigma-Aldrich, 99%) and chromium (III) chloride ($CrCl_3{\cdot}6H_2O$, Sigma-Aldrich, 96%) and citric acid (1:1) in distilled water (10 ml) and ethylene glycol (20 ml) while stirring and heating at 75 °C (1 h). A solution was dried in furnace at 80 °C for 12 h. A powder was made by heating the precursor to 700 °C for 1 h, Fig. 1a.

To produce PVC film, 2 g of polyvinyl chloride powder (PVC, Sigma-Aldrich) was dissolved in 100 ml tetrahydrofuran (THF) using a magnetic stirrer for 2 h at room temperature (RT). To make PVC/$FeCr_2O_4$/*x* wt% TPAI (x = 0, 2.5, 5, 10, 20), we repeated the prior step with varying concentrations of tetrapropylammonium iodide (TPAI, Sigma Aldrich, 98%) and/or 5 wt% $FeCr_2O_4$. After the solutions had formed, they were dried for two days in Petri dishes to create films, Fig. 1b. The resulting polymers have a thickness in the range 0.32–0.38 mm (as measured with a digital micrometer).

X-ray diffraction (X'Pert MPD, Philips, Cu-source) was utilized for analysis of the synthesized nanofiller ($FeCr_2O_4$), TPAI, and all polymers. MAUD software, which is based on the Rietveld method, was used to investigate the structure of $FeCr_2O_4$ (Lutterotti 2010; Rodríguez-Carvajal 1993).

All polymers were analyzed using Fourier transform infrared spectroscopy (Bruker Tensor 27 FTIR Spectrometer). Images of polymers' surfaces were captured by a JEOL (Akishima, Tokyo, Japan JED-2200 Series) scanning electron microscope. The UV diffuse reflectance (*R*), absorbance (*A*), and transmittance (*T*) of all polymers were measured using a JASCO-V-670 spectrophotometer with an integrating sphere assembly. The luminescence spectrophotometer (RF-1501 SHIMADZU, Ltd) was used to determine the fluorescence (FL) of each polymer. The optical band gap energies (E_g) were determined using (El-naggar et al. 2023a, b, c):

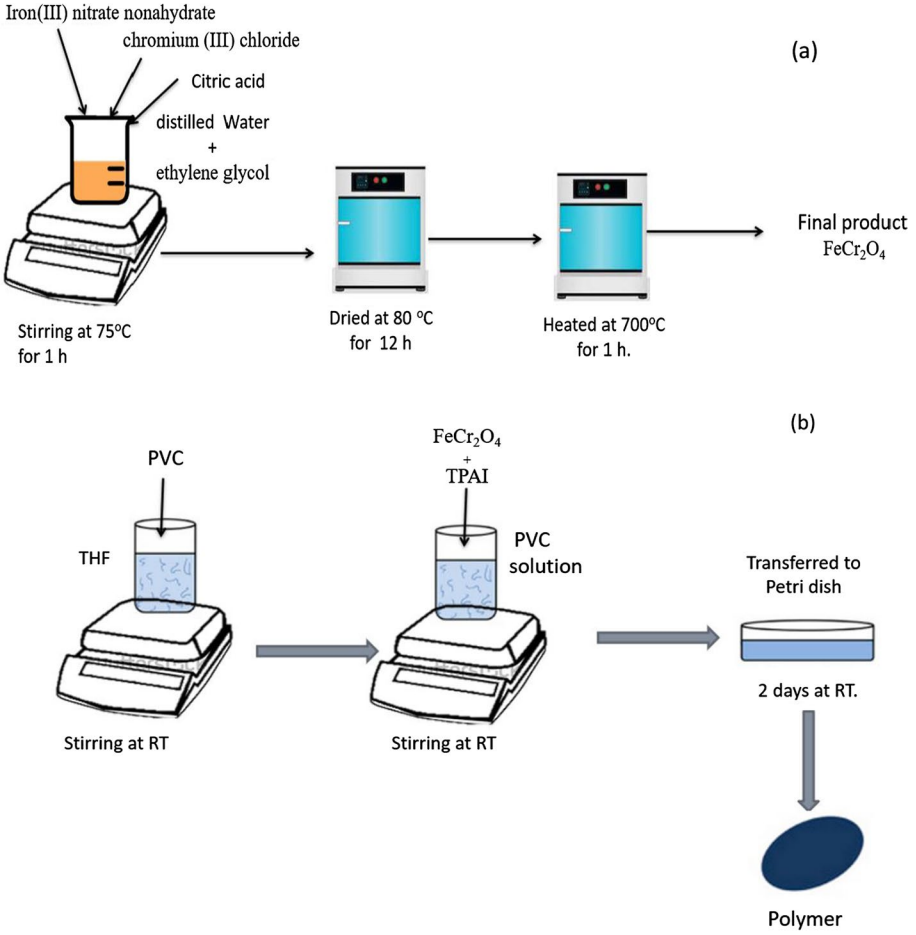

Fig. 1 Preparation schema for **a** $FeCr_2O_4$ filler and **b** PVC/$FeCr_2O_4$/10 wt% TPAI polymers

$$h\nu = H\left(h\nu - E_g\right)^m (1) \tag{1}$$

where h, *upsilon* f, H, $\alpha = 2.303$ A/t, A and t are Planck's constant, frequency of incident light, constant known as the disorder parameter, absorption coefficient, absorbance and thickness of each sample, respectively. $m = 0.5$ or 2 for direct and indirect transition, respectively.

The formula presented in Ref. (El-naggar et al. 2023a, b, c, d) was used to determine the linear optical parameters of all polymers.

The dielectric constant as a function of frequency ($f = 100$ Hz-1 MHz) at *RT* can be determined by applying an ac voltage of 2 V and measuring the resulting change in capacitance (C) and dissipation factor (tan δ). The following equations (El-Naggar et al. 2023a, b, c) were used to calculate the complex electric modulus ($M^* = M^{/} + iM^{//}$), ac conductivity (σ_{ac}), and dielectric constant (ε', ε'') of all polymers:

$$\epsilon' = \mathrm{dC}/\epsilon_0 \mathrm{A}(2)$$

$$\sigma_{ac} = 2\pi f \epsilon_0 \epsilon' \tan\delta \tag{3}$$

$$\tan\delta = \epsilon^{\cdot}/\epsilon' \tag{4}$$

$$M' = \frac{\epsilon'}{\epsilon^{\cdot 2} + \epsilon''^2} \tag{5}$$

$$M'' = \frac{\epsilon''}{\epsilon^{\cdot 2} + \epsilon''^2} \tag{6}$$

where ε_o, *and A* are the permittivity of free space and area of the disk, respectively.

3 Results and discussion

3.1 Structural investigation

The matching between the measured and calculated, from Rietveld refinement method, x ray diffraction patterns of $FeCr_2O_4$ powder is depicted in Fig. 2a. A single phase with cubic structure *Fd* 3 *m* was obtained with a cell parameter $a = 8.275(4)$ Å. The average crystallite size is in the nano range 9.4 nm with a little bit of a large lattice microstrain 0.0049. The x ray diffraction patterns obtained for the blend PVC/$FeCr_2O_4$/x% TPAI are given in Fig. 2b. The dominant amorphous phase of PVC was reflected in the high background of all XRD patterns, with weak diffraction peaks at 36.7 and 41.6° and two halos at approximately 15 and 17°, providing evidence of a little degree of crystallization. PVC has an orthorhombic unit cell and space group Pacm (Gilbert 1994). The crystalline syndiotactic isomer in the polymer is small compared to the amorphous atactic and isotactic isomers, so the diffracted intensity is low (Gilbert 1994; Brunner 1972). The diffraction data shows no significant differences between undoped and doped PVC with $FeCr_2O_4$, which may be due to its low contents or its uniform distribution. Lading TPAI up to 5% results in diffraction patterns similar to that of PVC doped with $FeCr_2O_4$ without any characteristic peaks from TPAI salt, indicating complete dissociation of the salt in the blend matrix. The undissociated salt, represented by the diffraction peaks of the TPAI salt, became more visible as the PVC was doped with a higher concentration of TPAI.

Figure 2c, d shows the SEM micrographs of undoped and doped PVC with $FeCr_2O_4$ and 10 wt% TPAI (as an example). As revealed from the graph the SEM image for PVC has a pore less and smooth surface. As $FeCr_2O_4$ and TPAI were added to PVC polymer, the film became rough, demonstrating the nanofiller's physical interaction with the host polymer (Yassin 2023).

A spectroscopic study relied on FT-IR data was applied at room temperature for PVC/$FeCr_2O_4$/TPAI samples. Figure 3 displays the FTIR transmittance data for unloaded and $FeCr_2O_4$ and/or TPAI-loaded PVC polymers. All polymers exhibit stretching of the C–Cl bond and vibrations of the carbonyl group at 792 and 1724 cm^{-1} (Mallakpour and Shamsaddinimotlagh 2018; Jia and Hu 2017; Chen et al. 2017). CH stretching, CH bending, and CH rocking vibrations are detected at 2922, 1401, and 1152 cm^{-1} in pure and doped PVC

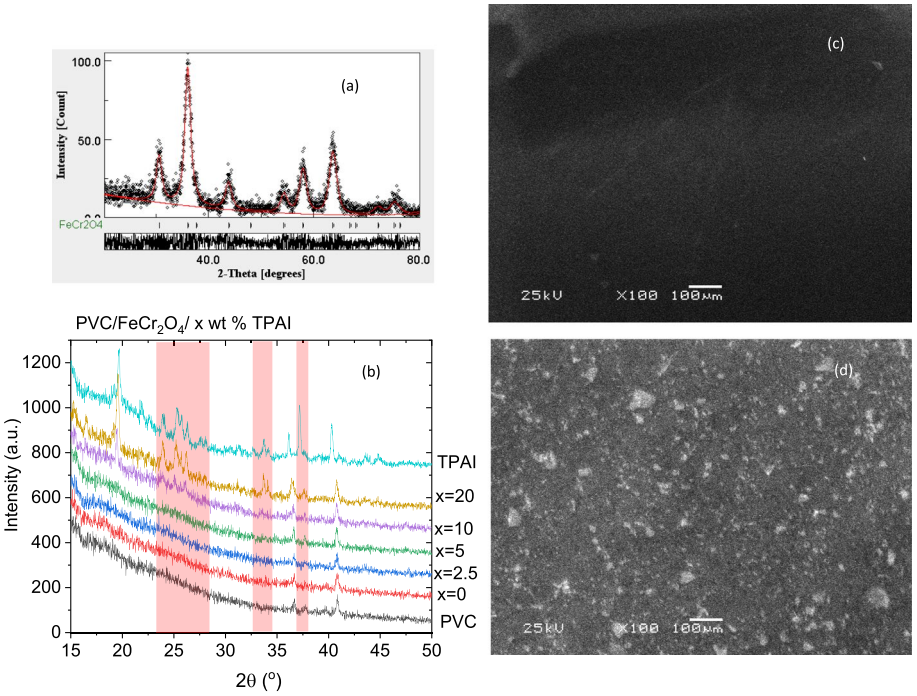

Fig. 2 **a** Rietveld refinement of $FeCr_2O_4$, **b** XRD diffraction data for undoped and doped PVC with $FeCr_2O_4$ and TPAI and **c**, **d** SEM patterns for PVC and PVC/$FeCr_2O_4$/10 wt % TPAI

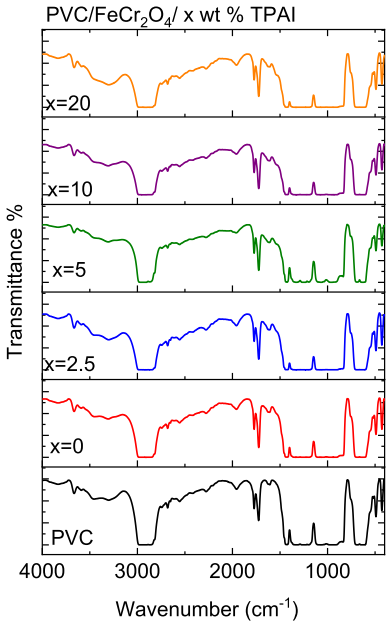

Fig. 3 FTIR data for undoped and doped PVC with $FeCr_2O_4$ and TPAI

polymers, respectively (Soman and Kelkar 2009; Rajendran et al. 2007). The peak positions and intensities of the vibration bands of PVC host polymer were slightly modified by doping. These shifts indicated that the host polymer and the filler were coupled. Yassin et al. argued these variation to the physicochemical interactions, of the host matrices which acting as electron donors and the filler which acting as electron acceptors (Yassin 2023).

3.2 Optical features

Measurements of PVC and PVC/$FeCr_2O_4$/*x* wt% TPAI polymers' diffused absorbance (*A*), transmittance (*T*), and reflectance (*R*) spectra are shown in Fig. 4. Figure 4a shows that all samples have two absorption peaks, at 232 and 283 nm, which are associated with electron transfer from $\pi \rightarrow \pi^*$ and $n \rightarrow \pi^*$ transitions owing to (C=C) unsaturated bonds and the C–Cl bond, respectively (Heiba et al. 2023). The graph shows that the absorbance spectrum of PVC polymer increased with the amount of $FeCr_2O_4$ loaded into the matrix and increased even more with the addition of TPAI. A similar result was detected in polyethylene oxide (PEO) and carboxymethyl cellulose (CMC) doped with ZnO/TiO_2 NPs (Taha 2019) or PVA doped with toluidine blue dye (Mohammed et al. 2022). After TPAI loading, the absorbance peaks shifted to longer wavelengths "red shifted," because of the TPAI's interaction with the polymer chains, which narrowed the optical band gap (Aziz et al.

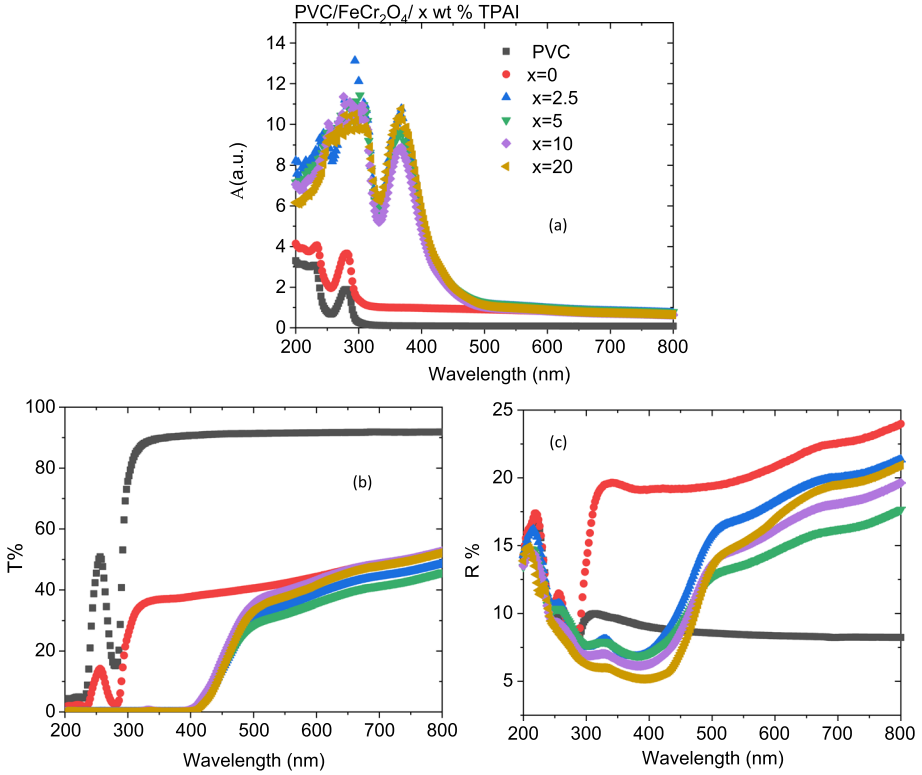

Fig. 4 **a** Absorbance, **b** transmittance and **c** reflectance spectra for undoped and doped PVC with $FeCr_2O_4$ and TPAI

2017; Zhao et al. 2021). Doped polymers have good absorbance in the wavelength up to 500 nm (UV and visible ranges) as demonstrated by the graph. These findings confirmed the potential for boosting industrial deployment of doped PVC in fields like coatings, adhesives, medicine, and solar cells. The difference in transmittance (T) between the doped and undoped PVC film is shown in Fig. 4b. In the range of 300–800 nm, 92% of light is transmitted through a PVC film. The transmittance becomes lower with the addition of different contents from TPAI and reached the lower value 42% as the amount of TPAI becomes 5 wt %. This correlates with the TPAI's high absorbency. Reflectance (R) spectra of the investigated samples are displayed in Fig. 4c, where the R% values demonstrate a significant increase following doping with $FeCr_2O_4$ and/or TPAI. At 500 nm, R increased from 9 to 19% as PVC doped with $FeCr_2O_4$ then it reduced to its lowest value (13%) as the amounts of TPAI became 5% in the polymer matrix. A similar result was observed when polyethylene oxide (PEO) doped with different I_2 concentrations (Telfah et al. 2022a, b).

All polymers' direct and indirect optical band gaps (E_g) were calculated using plots of $(\alpha h\nu)^2$ or $(\alpha h\nu)^{0.5}$ versus $h\nu$, respectively (Fig. 5). Extrapolating the linear portions of these plots until they intersected $h\nu = 0$ yielded the E_g values, Table 1. The obtained direct and indirect E_g values are (5.15, 4.26) and (4.95, 4.1) eV for PVC, respectively. Upon loading the PVC with $FeCr_2O_4$ the direct and indirect E_g values were reduced to (5, 4.23) and (4.95, 4.1) eV, respectively. After that they reduced further but irregularly as the amount

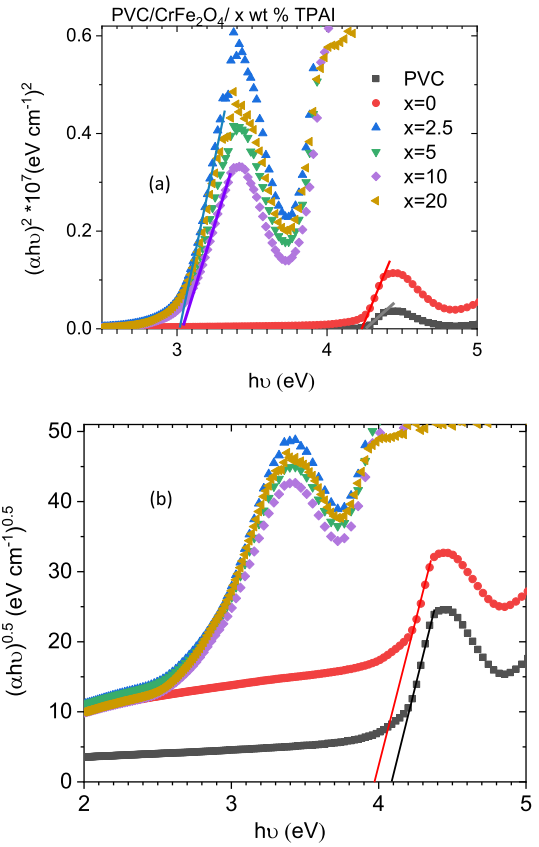

Fig. 5 Tauc relation for **a** direct and **b** indirect optical band gaps for undoped and doped PVC with $FeCr_2O_4$ and TPAI

Table 1 Direct and indirect optical band gap energies for undoped and doped PVC with $FeCr_2O_4$/TPAI

	Direct E_g (eV)	Indirect E_g (eV)
PVC	5.15, 4.26	4.95, 4.1
PVC/$FeCr_2O_4$/x wt % TPAI		
x = 0	5, 4.23	4.34, 3.87
x = 2.5	3.73, 2.98	3.11, 2.42
x = 5	3.82, 3.06	3.33, 2.55
x = 10	3.83, 3.08	3.34, 2.57
x = 20	3.81, 3.07	3.32, 2.56

of TPAI doing increased reached their lowest values (3.73, 2.98) and (3.11, 2.42) eV for direct and indirect transition as the amounts of TPAI became 2.5 wt%. A similar result was observed for PVC doped with iodine (Telfah et al. 2022a, b). The optical band gap of the host material is narrowed when it is loaded with nanofillers because new localized energy states are formed between the highest occupied molecular orbital (HOMO) and the lowest unoccupied molecular orbital (LUMO) levels (El-naggar et al. 2022a, b, c).

Figure 6 displays the results of an investigation into how $FeCr_2O_4$ and/or TPAI affect the extinction coefficient (k) and refractive index (n) of PVC. As can be seen, the k value increased with doped PVC with $FeCr_2O_4$ and increased further as the amount of TPAI increased in the host polymer, reaching its highest value as the amount of TPAI became 2.5 wt%, Fig. 6a. The reaction between light and medium molecules causes energy loss, which leads to a higher k value and a higher absorption coefficient in the material (Abdel-Kader et al. 2023). Furthermore, the value of n of PVC increased as it loaded with $FeCr_2O_4$ and it increased further as it loaded with TPAI in the whole wavelength except at $\lambda = 300–450$ nm, the situation is reversed. When different fillers are added to PVC, the host polymer's polarizability changes, as indicated by a change in the packing density, or n value (El-naggar et al. 2022a, b, c). Increases or decreases in the value of n in the doped polymer may be linked to modifications to the polymer's structure, which in turn may have a significant impact on the films' varying physical properties. The investigated polymers have potential for use in polymer-optoelectronics, highly reflective fields, and strong optical confinement (Aziz et al. 2015).

Figure 7 depicts the change in the dielectric constant (real ε_r and imaginary ε_i) parts and the (surface, volume) energy loss functions (SELF, VELF) of PVC polymer caused by the addition of $FeCr_2O_4$ and/or TPAI filler. Similar behaviors are seen between the real part (ε_r) and imaginary part (ε_i) of the dielectric constant and the refractive index and extinction coefficient. The sample's reflectance had an effect on the n values, while the sample's absorbance determined the k values. It is claimed that the nature of the nanofillers is what causes some peaks to appear in measurements of dielectric. Additionally, in each sample, the VELF values are higher than the corresponding SELF values. Furthermore, in the visible range, PVC polymer with $FeCr_2O_4$ has the highest ε_r value while PVC doped polymers with $FeCr_2O_4$ and TPAI have the highest (ε_i, SELF, VELF) values. The following changes may be response for changes in the dielectric constant upon loading with various fillers:

(i) The alteration in the interaction between the incident photon and the electron in the nanofillers and (ii) the variations in the dipole motion of the doped polymer as compared with undoped one, respectively (Suma et al. 2017).

The optical conductivity (σ_{opt}) of undoped and doped PVC polymers was calculated using the absorption coefficient and refractive index n (Fig. 8). σ_{opt} rose as PVC doped with

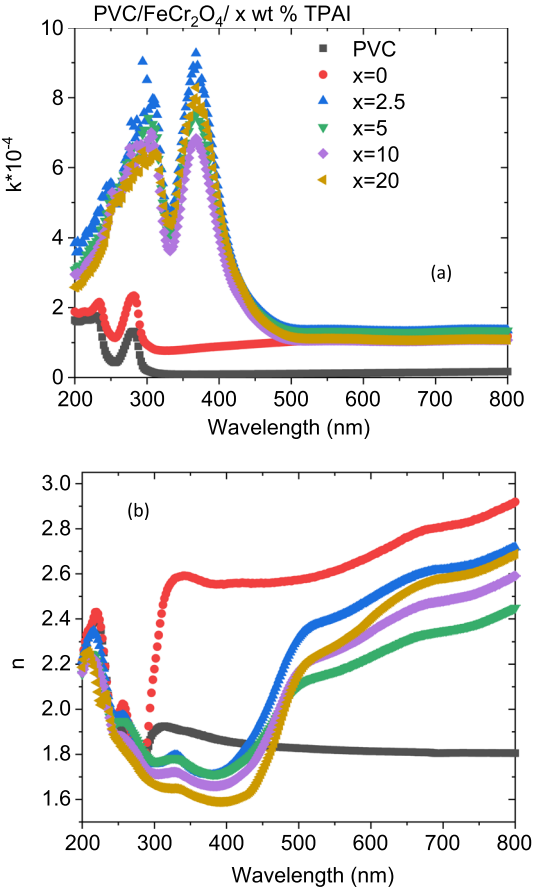

Fig. 6 **a** Refractive index and **b** extinction coefficient as function of the wavelength for undoped and doped PVC with $FeCr_2O_4$ and TPAI

$FeCr_2O_4$ and rose further as it loaded with TPAI. σ_{opt} values are thought to have risen as a result of a higher rate of photon absorption, which increased the number of electrons that were produced (Ismail et al. 2022).

The effect of $FeCr_2O_4$ and/or TPAI filler on the first- order linear optical susceptibility ($\chi^{(1)}$), third-order nonlinear susceptibility ($\chi^{(3)}$) and nonlinear refractive index (n_2) of PVC polymer has been studied. When an electric field is applied, a polarization process takes place that results in nonlinear optical parameters (Erken 2022). Figure 9 depicts the three parameters under consideration. All three parameters for all polymers followed the same general pattern. In addition, all three values are greater than what is seen in a polymer made entirely of PVC. PVC filled with $FeCr_2O_4$ only has the highest non-linear optical (NLO) parameters. A similar result was detected as PVA/PVP polymeric blends doped with potassium dichromate (AlAbdulaal et al. 2023). As PVC/$FeCr_2O_4$ doped with TPAI, the NLO parameters decreased irregularly. Variations in the polymer absorption process due to filler type are largely responsible for these findings. Doped polymers have been recommended for use in photonic and optical applications due to their achieved nonlinear optical features.

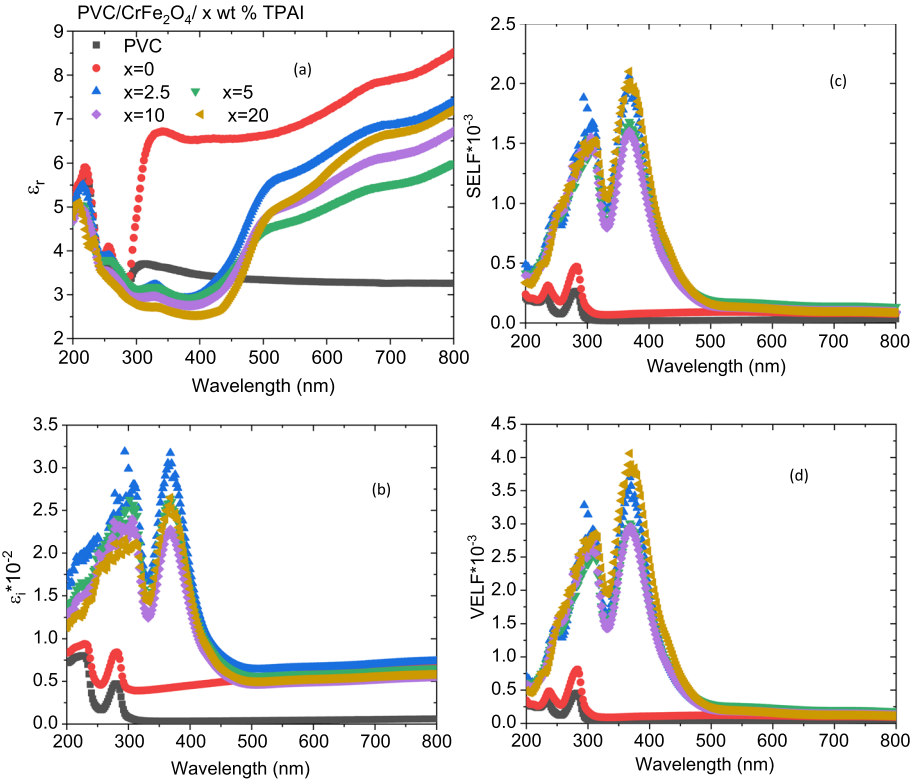

Fig. 7 The altering of **a** real and **b** imaginary dielectric constant, **c** SELF and **d** VELF with the wavelength for undoped and doped PVC with $FeCr_2O_4$ and TPAI

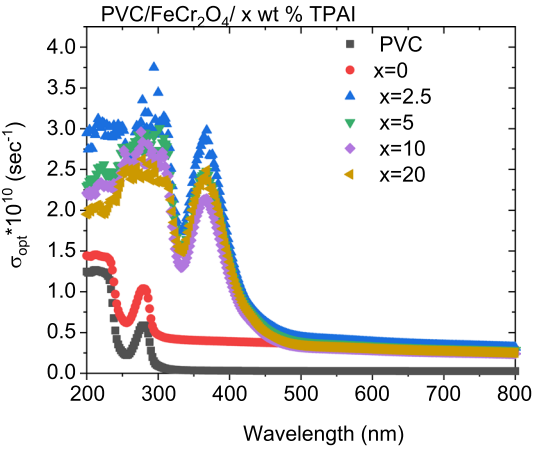

Fig. 8 Optical conductivity for undoped and doped PVC with $FeCr_2O_4$ and TPAI

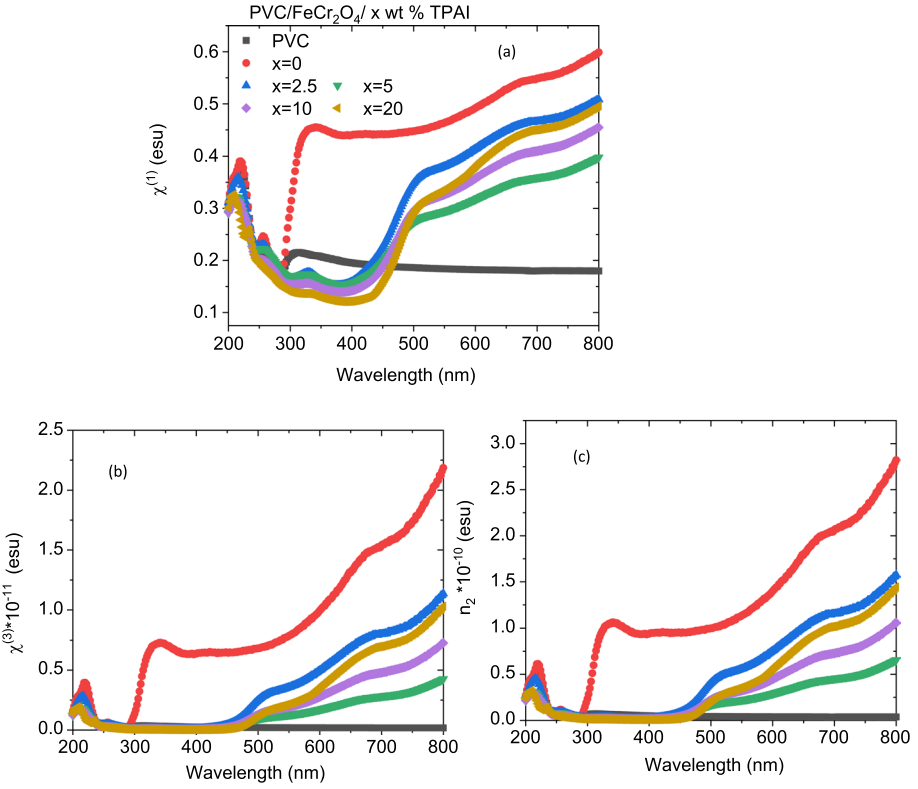

Fig. 9 **a–c** Wavelength dependent of the nonlinear optical parameters for undoped and doped PVC with $FeCr_2O_4$ and TPAI

3.3 Fluorescence analysis

The FL emission spectra measured under different excitation wavelengths, λ_{exc}=317, 380, and 434 nm, are shown in Fig. 10 for pure PVC and loaded with $FeCr_2O_4$/x w% TPAI. The emission band appeared at 397 nm is characteristic of PVC excimer fluorescence through the π*–π electronic transition (El–Hachemi et al. 2021). This characteristic band is shifted to 405 and 468 nm under λ_{exc}=380 and 434 nm excitation wavelengths. The shoulder peaks appeared at 428 and 382 nm may be assigned to trapped energy levels arising from defect impurities, or π*– *n* transition (El–Hachemi et al. 2021).

The FL intensity of pure PVC polymer is obviously quenched upon loading with $FeCr_2O_4$ and further decreased a little by adding 0.05% TPAI to PVC; further increasing the TPAI content did not affect the FL intensity. Fluorescence quenching may occur by a variety of molecular interactions with quencher molecule(s) such as: excited-state reactions, molecular rearrangements, energy transfer, ground-state complex formation, and collisional quenching (Lakowicz 2006). The polymer (organic) and the $CrFe_2O_4$ (inorganic) components may interact by Förster resonant energy transfer (FRET) and/or electron transfer toward the nanocrystals (NCs) depending on the relative values of the energy gap and on the surface functionalization of the NCs, resulting in exciton quenching in the polymer

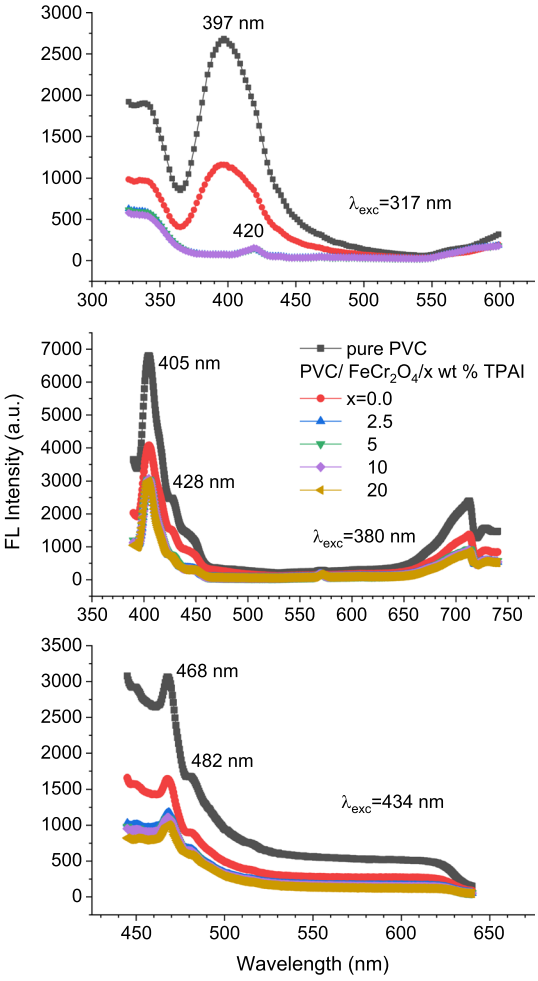

Fig. 10 FL spectra for undoped and doped PVC with $FeCr_2O_4$ and TPAI under different excitation wavelengths

(Anni 2019). For FRET to be takes place, a good overlap between the polymer photoluminescence range and the NCs absorption one should be fulfilled (Anni 2019), which is realized between PVC and $FeCr_2O_4$. The existence of the NCs in the polymer presented an additional decay channel for the photogenerated excitons in the polymer. Upon loading TPAI, interaction between PVC and TPAI molecules may occur resulting in delocalization in PVC. TPAI may connect with one or more PVC polymer repeating units forming trap sites obstructing the electron-hole recombination process. The decrease in FL emission implies inhibited recombination of photogenerated charge carriers for the present system, which nominates it for photocatalytic applications.

The emitted colors from different samples have also been described using color coordinates derived from the CIE 1931 chromaticity diagram (Fig. 11). Under excitation wavelengths of 317, 380, and 434 nm, respectively, the estimated color coordinates of normalized PVC were (0.1997, 0.0797), (0.2113, 0.0552), and (0.2202, 0.2147), all

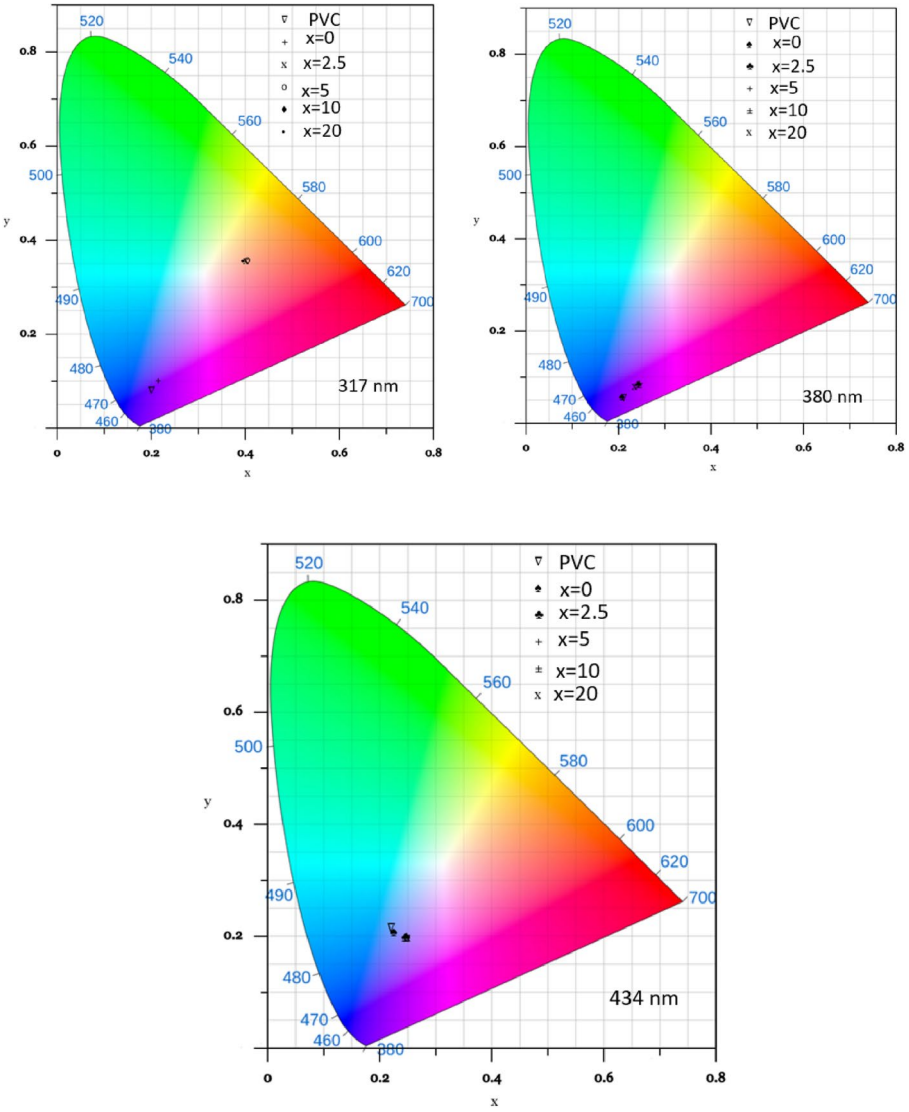

Fig. 11 CIE diagram for undoped and doped PVC with $FeCr_2O_4$ and TPAI under different excitation wavelengths

Table 2 Chromaticity coordinates (x, y) for the FL spectra denoted in Fig. 10

	317 nm	380 nm	434 nm
PVC	(0.1997, 0.0797)	(0.2113, 0.0552)	(0.2202, 0.2147)
PVC/$FeCr_2O_4$/x wt % TPAI			
x = 0	(0.2143, 0.1007)	(0.2065, 0.0569)	(0.2246, 0.2072)
x = 2.5	(0.4020, 0.3556)	(0.2408, 0.0835)	(0.2452, 0.1980)
x = 5	(0.4054, 0.3576)	(0.2450, 0.0868)	(0.2468, 0.2011)
x = 10	(0.4026, 0.3572)	(0.2428, 0.0843)	(0.2440, 0.1983)
x = 20	(0.3970, 0.3561)	(0.2350, 0.0795)	(0.2492, 0.1975)

of which correspond to blue-violet emission. Except for $FeCr_2O_4$ and TPAI-doped PVC, which showed orange emission under 317 nm, the emission from doped PVC with the fillers clearly exhibited a blue-violet emission under the different excitation wavelengths. The obtained sample color coordinates are presented in Table 2. The current system may even have practical implications for LED use in industry.

3.4 Dielectric characteristics

The frequency (Log *f*) dependence of the real and imaginary parts of the dielectric constant (ε', ε'') for undoped and doped PVC polymers is shown in Fig. 12a, b. The interfacial effect

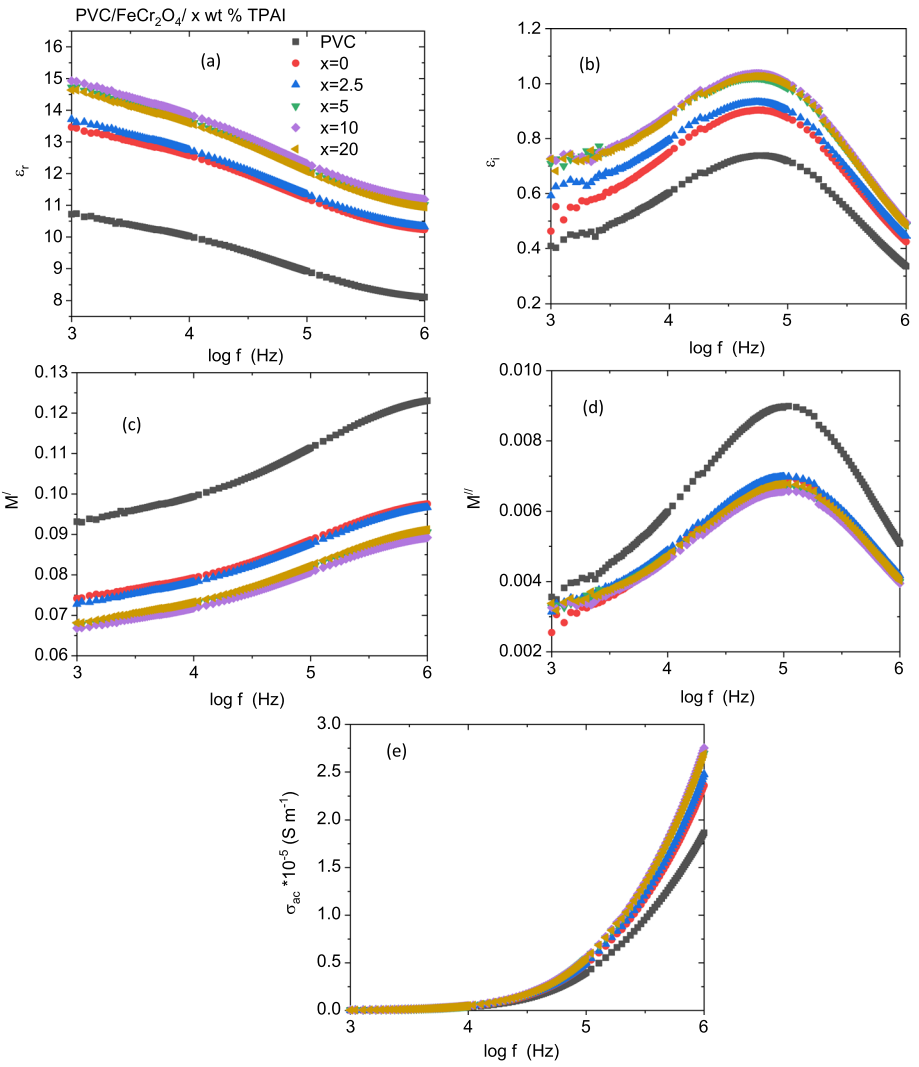

Fig. 12 Changing of the **a** real, **b** imaginary dielectric constant, **c** real, **d** imaginary parts of electric modulus and **e** ac conductivity for undoped and doped PVC with $FeCr_2O_4$ and TPAI

between the polymer and electrode causes ε' values to be relatively high at low frequencies. Dipoles in polymeric films aligned with the applied field's direction, resulting in a decrease in ε' values as frequency was raised for all samples. The ε'' value increased with increasing frequency for all polymers up to a maximum value, after which it decreased with increasing frequency. The peaks' locations are altered as PVC doped with $FeCr_2O_4$ and/or TPAI. This change is suggestive of a different relaxation time (Bharati et al. 2016). The values ε' and ε'' were increased as PVC loaded with $FeCr_2O_4$. Similar results were observed as PVA doped with toluidine blue dye or PVA/PEG doped with the methyl blue dye (Mohammed et al. 2022, 2023). In contrast the dielectric const was decreased as PEO/CMC doped with ZnO/TiO_2 (Ragab 2023). Upon loaded PVC/$FeCr_2O_4$ polymer with TPAI, both ε' and ε'' increased irregularly, reached their maximum values as the amount of TPAI became 10 wt %. The increasing in the ε' value may be caused by the changes in the order distribution of $FeCr_2O_4$ and/or TPAI on the PVC polymer, which in turn alters the interfacial polarization (Mohamed et al. 2014). Therefore, the incorporating of the fillers into the PVC had a beneficial influence on enhancing in the dielectric features of the host PVC, confirming the XRD and UV–Vis results. A similar result was observed as PVP/PVA/CMC blend was loaded with AuNPs (Yassin 2023). This increasing in the dielectric values can nominated the doped polymer to utilized in applications of polymer based capacitors in the energy storage devices (Al-Muntaser et al. 2023).

Due to the fact that the electric modulus formalism allows for the neglect of electrode polarization, absorption, and impurity interactions, large deviations in the components of complex dielectric permittivity can be decreased. Electric modulus (M', M'') real and imaginary parts as a function of frequency are shown for all polymers in Fig. 12c, d. The graph clearly shows that M' is very small at low frequencies. PVC's M' reduced as it was loaded with $FeCr_2O_4$ and reduced further as it doped with TPAI. Similar result was observed as PVA doped with toluidine blue dye (Mohammed et al. 2022). Based on these results, it appeared that electrode polarization and electrode effects were relatively unimportant (Howell et al. 1974). Also, the lessening in M' values, at low frequency range, found as a result of integrating the $FeCr_2O_4$ and TPAI into the PVC polymer proposes that triggered electrons hop from one place to another. This finding approves that hopping is the foremost conduction mechanism in the system under study The values of M' increased along with the frequency. In the presence of more efficient interfacial polarization (Naik et al. 2016), higher-frequency unsaturation values were noticed. Furthermore, M'' displayed a peak in all polymers. The intensity of this peak was reduced as PVC loaded with $CrFe_2O_4$ and/or TPAI and the position of this peak affected by $FeCr_2O_4$ and /or TPAI.

Figure 12e shows the frequency dependence of the AC conductivity (σ_{ac}) for both undoped and doped PVC using the $FeCr_2O_4$ and/or TPAI system. All polymers followed the same pattern, with σ_{ac} growing larger as frequency did. This increase in σ_{ac} is caused by an increase in electron hopping at relatively high frequencies. Doping PVC with $FeCr_2O_4$ resulted in a rise in AC conductivity, which was further bolstered by the addition of TPAI. Similar result was detected as PEO/CMC doped with ZnO/TiO_2 (Ragab 2023). Changes in AC conductivity as PVC may result from a change in the number of charge carriers and surface defects caused by the interaction between $FeCr_2O_4$ and TPAI within the polymer matrix (Abdelhamied et al. 2022).

4 Conclusion

$FeCr_2O_4$ with a single-phase cubic structure $Fd\bar{3}m$, average crystallite size 9.4 nm was used as nanofiller for PVC polymer. PVC films, ~0.35 mm, loaded with $FeCr_2O_4$ and different wt% of TPAI ($x=0$, 2.5, 5, 10, 20) were produced with uniform distribution of the nanofiller in PVC matrixî. Doped polymers had good absorbance in wavelengths up to 500 nm (UV and visible ranges) nominating it in several fields like coatings, adhesives, medicine, and solar cells. For wavelengths ≥ 330 nm, R and n enhanced greatly when PVC doped with $FeCr_2O_4$, both reduced with TPAI doping in the range $\lambda=300$–450 nm and increased again for $\lambda \geq 460$ nm. Both k and σ_{opt} were increased when doping PVC with $FeCr_2O_4$ and increased further as the amount of TPAI increased, reaching highest values for TPAI 2.5 wt%. The doped polymers have potential for use in polymer-optoelectronics, highly reflective fields, and strong optical confinement. In the visible range, PVC/$FeCr_2O_4$ has the highest ε_r value while PVC/$FeCr_2O_4$/TPAI have the highest (ε_i, SELF, VELF) values. Such improvements in nonlinear optical features recommend present composite for use in photonic and optical applications. $FeCr_2O_4$ molecules acted as fluorescence quencher and reduced the FL intensity of pure PVC polymer. Loading TPAI to PVC produced little effect on the FL intensity. Except for $FeCr_2O_4$ and TPAI-doped PVC, which showed orange emission under 317 nm, the emission from undoped and doped PVC with the fillers clearly exhibited a blue-violet emission under the different excitation wavelengths. The values ε' and ε'' were increased as PVC loaded with $FeCr_2O_4$. Upon loaded PVC/$FeCr_2O_4$ polymer with TPAI, both ε' and ε'' increased irregularly, reached their maximum values as the amount of TPAI became 10 wt %. Doping PVC with $FeCr_2O_4$ resulted in a rise in AC conductivity, which was further bolstered by the addition of TPAI. The enhanced dielectric properties of PVC/$FeCr_2O_4$/TPAI nominated them to be used in different optoelectronic applications such as sensors and as polymer based capacitors in the energy storage devices.

Acknowledgements The authors extend their appreciation to the Deputyship for Research & Innovation, Ministry of Education in Saudi Arabia for funding this research. (IFKSURC-1-1018).

Author contributions All authors have contributed, discussed the results and approved the final manuscript.

Funding the Deputyship for Research & Innovation, Ministry of Education in Saudi Arabia.

Data availability The authors confirm that the data supporting the findings of this study are available within the article.

Declarations

Conflict of interest The authors declare no competing interests.

Ethical approval We agreed on all terms and conditions for ethics approval.

References

Abdel Maksoud, M.I.A., Bekhit, M., Waly c, A.L., Awed, A.S.: Optical and dielectric properties of polymer nanocomposite based on PVC matrix and Cu/Cu2O. Phys. E **148**, 115661 (2023)

Abdel-Kader, M.H., Mohamed, A.A.H., Mohamed, M.B.: Effect of laser irradiation on structural, linear and nonlinear optical characteristics of PVP/CMC/ZnS–NiO blends. J. Laser Appl. **35**(2), 022026 (2023)

Abdelhamied, M.M., Abdelreheem, A.M., Atta, A.: Influence of ion beam and silver nanoparticles on dielectric properties of flexible PVA/PANI polymer composite films. Plast. Rubber Compos. **51**(1), 1 (2022)

Al-Muntaser, A.A., Abdelghany, A.M., Abdelrazek, E.M., Elshahawy, A.G.: Enhancement of optical and electrical properties of PVC/PMMA blend films doped with $Li_4Ti_5O_{12}$ nanoparticles. J. Mater. Sci. Technol. **9**(1), 789 (2020)

Al-Muntaser, A.A., Pashameah, R.A., Saeed, A., Alwafi, R., Alzahrani, E., AlSubhi, S.A., Yassin, A.Y.: Boosting the optical, structural, electrical, and dielectric properties of polystyrene using a hybrid GNP/Cu nanofiller: novel nanocomposites for energy storage applications. J. Mater. Sci. Mater. Electron. **34**, 678 (2023)

AlAbdulaal, T.H., Almoadi, A., Yahia, I.S., Zahran, H.Y., Alqahtani, M.S., Yousef, E.S., Alahmari, S., Jalalah, M., Harraz, F.A., Al-Assiri, M.S.: Effects of potassium dichromate on the structural, linear/nonlinear optical properties of the fabricated PVA/PVP polymeric blends: for optoelectronics. Mater. Sci. Eng. B **292**, 116364 (2023)

Alhulw, H., Alshammari, T.A., Taha: Structure, thermal and dielectric insights of PVC/PVP/ZnFe2O4 polymer nanocomposites. Eur. Phys. J. Plus **136**, 1201 (2021)

Anni, M.: Polymer-II-VI nanocrystals blends: basic physics and device applications to lasers and LEDs. Nanomaterials **9**, 1036 (2019)

Anum, R., Zahid, M., Siddique, S., Fayzan Shakir, H.M., Rehan, Z.A.: PVC based flexible nanocomposites with the incorporation of polyaniline and barium hexa-ferrite nanoparticles for the shielding against EMI, NIR, and thermal imaging cameras. Synth. Met. **277**, 116773 (2021)

Aziz, S.B., Ahmed, H.M., Hussein, A.M., Fathulla, A.B., Wsw, R.M., Hussein, R.T.: Tuning the absorption of ultraviolet spectra and optical parameters of aluminum doped PVA based solid polymer composites. J. Mater. Sci. Mater. Electron. **26**, 8022 (2015)

Aziz, S.B., Rasheed, M.A., Ahmed, H.M.: Synthesis of polymer nanocomposites based on [methyl cellulose](1 – x):(CuS)x (0.02 M ≤ x ≤ 0.08 M) with desired optical band gaps. Polym. (Basel) **9**(6), 194 (2017)

Bera, S., Singh, M., Thantirige, R., Tiwary, S.K., Shook, B.T., Nieves, E., Raghavan, D., Karim, A.: Pradhan, 2D-nanofiller-based polymer nanocomposites for capacitive energy storage applications. Small Sci. **2300016**, 1 (2023)

Bharati, A., Wübbenhorst, M., Moldenaers, P., Cardinaels, R.: Effect of compatibilization on interfacial polarization and intrinsic length scales in biphasic polymer blends of PαMSAN and PMMA: a combined experimental and modeling dielectric study. Macromolecules **49**, 1464 (2016)

Brunner, A.J.: X-ray diffraction pattern of poly(vinyl chloride). Polym. Lett. **10**, 379 (1972)

Chen, J., Nie, X.A., Jiang, J.C., Zhou, Y.H.: Thermal degradation and plasticizing mechanism of poly(vinyl chloride) plasticized with a novel cardanol derived plasticizer. IOP Conf. Ser. Mater. Sci. Eng. **292**, 01200 (2017)

Dippong, T., Deac, I.G., Cadar, O., Levei, E.A.: Effect of silica embedding on the structure, morphology and magnetic behavior of (Zn0.6Mn0.4Fe2O4)δ/(SiO2)(100-δ) nanoparticles. Nanomaterials **11**, 2232 (2021)

El-naggar, A.M., Alsaggaf, A., Heiba, Z.K., Kamal, A.M., Aldhafiri, A.M., Fatehmulla, A., Mohamed, M.B.: Exploring the structural, optical and electrical characteristics of PVA/PANi blends. Opt. Mater. **139**, 113771 (2023)

El-naggar, A.M., Alsaggaf, A., Heiba, Z.K., Kamal, A.M., Aldhafiri, A.M., Mohamed, M.B.: Impact of MWCNTs on the structural, electrical, and optical characteristics of PVA/PANi blends. J. Taibah Univ. Sci. **17**(1), 2207769 (2023)

El-naggar, A.M., Heiba, Z.K., Kamal, A.M., Abd-Elkader, O.H., Lakshminarayana, G., Mohamed, M.B.: Linear and nonlinear optical characteristics of PVA/CMC/PEG blended polymer loaded with ZnS formed at different temperatures. J. Mater. Sci. Mater. Electron. **34**(2), 114 (2023)

El-Naggar, A.M., Heiba, Z.K., Kamal, A.M., Abd-Elkader, O.H., Mohamed, M.B.: Impact of ZnS/Mn on the structure optical and electric properties of PVC polymer. Polymers **15**(9), 2091 (2023)

El-Naggar, A.M., Heiba, Z.K., Kamal, A.M., Abd-Elkader, O.H., Mohamed, M.B.: Structural, optical, and dielectric performance of PVA/PVP/PEG blend loaded with nano CoFe2 – xErxO4 ferrite. J. Mater. Sci. Mater. Electron. **34**(6), 566 (2023)

El-naggar, A.M., Heiba, Z.K., Mohamed, M.B., Kamal, A.M., Abd-Elkader, O.H., Lakshminarayana, G.: Effect of ZnO/(Co or Mn) ratios on the structure and optical spectroscopy parameters of PVA/PVP/PEG blended polymer. Opt. Mater. **128**, 112411 (2022)

El-naggar, A.M., Heiba, Z.K., Mohamed, M.B., Kamal, A.M., Lakshminarayana, G., Abd-Elkader, O.H.: Effect of MnS/ZnS nanocomposite on the structural, linear and nonlinear optical properties of PVA/CMC blended polymer. Opt. Mater. **128**, 112379 (2022)

El-naggar, A.M., Heiba, Z.K., Mohamed, M.B., Kamal, A.M., Lakshminarayana, G., Shar, M.A.: Muhammad Ali Shar, Structural, linear and nonlinear optical properties of poly(vinyl alcohol) (PVA)/polyethylene glycol (PEG)/SnS2: Y nanocomposite films. Optik **258**, 168941 (2022)

El–Hachemi, B., Miloud, S., MSabah, T., Souad, O., Zineddine, B., Boubekeur, S.M., Toufik: Halimi, Ouahiba, electrical and optical properties of PVC/ZnTe nanocomposite thin films. Inorg. Organomet. Polym. **31**, 3637 (2021)

Erken, O.: Effect of cycle numbers on the structural, linear and nonlinear optical properties in Fe2O3 thin films deposited by SILAR method. Curr. Appl. Phys. **34**, 7 (2022)

Gilbert, M.: Crystallinity in poly(vinyl chloride). Polym. Rev. **34**(1), 77 (1994)

Heiba, Z.K., BMohamed, M., Mostafa, N.Y.: El-Naggar, Structural and optical properties of Cd1–xMnxFe2O4/PMMA nanocomposites. J. Inorg. Organomet. Polym. **30**, 1898 (2020)

Heiba, Z.K., El-naggar, A.M., Kamal, A.M., Abd-Elkader, O.H., Mohamed, M.B.: Optical and dielectric properties of PVC/TiO2/TBAI ionic liquid polymer electrolyte. Opt. Mater. **139**, 113764 (2023)

Howell, F.S., Bose, R.A., Macedo, P.B., Moynihan, C.T.: Electrical relaxation in a glass-forming molten salt. J. Phys. Chem. **78**(6), 639 (1974)

Ismail, M.S., Elamin, A.A., Abdel-Wahab, F., Elbashar, Y.H., Mahasen, M.M.: Improving the refractive index by engineering PbS/PVA nano polymer composite for optoelectronic applications. Opt. Mater. **131**, 112639 (2022)

Jia, P., Hu, M.Z.L.: Cardanol groups grafted on poly(vinyl chloride)—synthesis, perfor-mance and plasticization mechanism. Polymers **9**, 621 (2017)

Khan, M.Z.H., Al-Mamun, M.R., Halder, P.K., Aziz, M.A.: Renew. Sust Energ. Rev. **71**, 602 (2017)

Lakowicz, J.R.: Quenching of fluorescence. In: Principles of Fluorescence Spectroscopy. Springer, Boston, MA (2006)

Lutterotti, L.: Total pattern fitting for the combined size–strain–stress–texture determination in thin film diffraction. Nucl. Inst. Methods Phys. Res. B **268**, 334 (2010)

Mallakpour, S., Shamsaddinimotlagh, S.: Ultrasonic-promoted rapid preparation of PVC/TiO2-BSA nanocomposites: characterization and photocatalytic degradation of methylene blue. Ultrason. Sonochem. **41**, 361 (2018)

Mohamed, S.A., Al-Ghamdi, A.A., Sharma, G.D., Mansy, M.K.E.: Effect of ethylene carbonate as a plasticizer on CuI/PVA nanocomposite: structure, optical and electrical properties. J. Adv. Res. **5**, 79 (2014)

Mohammed, M.I., Yahia, I.S., Abd El-Mongy, S.: Simple fabrication of PVA/PEG blend doped with methyl blue dye with superior optical limiting performance: enhanced luminescence property, structural, and dielectric properties. Mater. Sci .Eng. B **291**, 116390 (2023)

Mohammed, M.I., Yahia, I.S., Salem, G.F.: Design of a smart optical sensor employing Toluidine Blue dye as an effective laser optical limiter integrated into (PVA) composite films: electrical conductivity and dielectric characteristics improvement. Opt. Laser Technol. **156**, 108629 (2022)

Mubasher, M., Mumtaz, M., Hassan, N.U.R., Lashari, Z., Ahmad, M.T., Khan, M., Ali: Synthesis and cyclic voltammetry of CrFe2O4/(MWCNTs)x nanohybrids. J. Mater. Sci. Mater. Electron. **31**, 13909 (2020)

Naik, J., Bhajantri, R.F., Rathod, S.G., Sheela, T., Ravindrachary, V.: Synthesis and characterization of multifunctional ZnBr2/PVA polymer dielectrics. J. Adv. Dielectr. **06**(04), 1650028 (2016)

Ragab, H.M.: Optical, thermal and electrical characterization of PEO/CMC incorporated with ZnO/TiO2 NPs for advanced flexible optoelectronic technologies. Ceram. Int. **49**, 12563 (2023)

Rajendran, S., Sivakumar, P., Babu, R.S.: Studies on the salt concentration of a PVdF–PVC based polymer blend electrolyte. J Power Source **164**, 815 (2007)

Rodríguez-Carvajal, J.: Recent advances in magnetic structure determination by neutron powder diffraction. Phys. B (Amst. Neth.) **192**, 55 (1993)

Singh, K., Maignan, A., Simon, C., Martin, C.: FeCr2O4 and CoCr2O4 spinels: multiferroicity in the collinear magnetic state. Appl Phys Lett **99**, 172903 (2011)

Soliman, T.S., Abouhaswa, A.S.: Synthesis and structural of Cd0.5Zn0.5F2O4 nanoparticles and its influence on the structure and optical properties of polyvinyl alcohol films. J. Mater. Sci. Mater. Electron **31**, 9666 (2020)

Soman, V.V., Kelkar, D.S.: FTIR studies of doped PMMA–PVC blend system. Macromol. Symp. **277**, 152 (2009)

Suma, G.R., Subramani, N.K., Shilpa, K.N., Sachhidananda, S., Satyanarayana, S.V.: Effect of Ce0.5Zr0.5O2 nano fillers on structural and optical behaviors of poly(vinyl alcohol). J. Mater. Sci. Mater. Electron **28**(14), 10707 (2017)

Suvaran, S., Niranjana, V.S., Subburaj, M., Ramesan, M.T.: Temperature-dependent conductivity, optical properties, thermal stability and dielectric modelling studies of Cu-Al2O3/CPE/PVC blend nanocomposites. Bull. Mater. Sci. **45**, 246 (2022)

Taha, T.A.: Optical properties of PVC/Al2O3 nanocomposite films. Polym. Bull. **76**, 903 (2019)

Taha, T.A., Hendawy, N., El–Rabaie, S., Esmat, A.: El–Mansy, Effect of NiO NPs doping on the structure and optical properties of PVC polymer films. Polym. Bull. **76**, 4769 (2019)
Telfah, M., Ahmad, A.A., Alsaad, A.M., Al–Bataineh, Q.M., Telfah, A.: Doping mechanism and optical properties of as–prepared polyvinyl chloride (PVC) doped by iodine thin films. Polym. Bull. **79**, 10803 (2022)
Telfah, A., Al–Bataineh, Q.M., Tolstik, E., Ahmad, A.A., Alsaad, A.M., Ababneh, R., Tavares, C.J., Hergenröder, R.: Opticlectrical and chemical properties of PEO: I2 complex composite films, Polym. Bull. (2022) https://doi.org/10.1007/s00289-022-04508-4
Yassin, A.Y.: Dielectric spectroscopy characterization of relaxation in composite based on (PVA–PVP) blend for nickel–cadmium batteries. J. Mater. Sci. Mater. Electron. **31**, 19447 (2020)
Yassin, A.Y.: Synthesized polymeric nanocomposites with enhanced optical and electrical properties based on gold nanoparticles for optoelectronic applications. J. Mater. Sci. Mater. Electron **34**, 46 (2023)
Yee, L.P., Farhana, N.K., Omar, F.S., Sundararajan, V., Bashir, S., Saidi, N.M., Ramesh, S., Ramesh, K.: Enhancing efficiency of dye sensitized solar cells based on poly(propylene) carbonate polymer gel electrolytes incorporating double salts. Ionics **26**(1), 493 (2020)
Zhao, Y., Zuo, Y., He, G., Chen, Q., Meng, Q., Chen, H.: Synthesis of graphene-based CdS@CuS core-shell nanorods by cation-exchange for efficient degradation of ciprofloxacin. J. Alloys Compd. **869**, 159305 (2021)

Publisher's Note Springer Nature remains neutral with regard to jurisdictional claims in published maps and institutional affiliations.

Springer Nature or its licensor (e.g. a society or other partner) holds exclusive rights to this article under a publishing agreement with the author(s) or other rightsholder(s); author self-archiving of the accepted manuscript version of this article is solely governed by the terms of such publishing agreement and applicable law.